PCCP

Accepted Manuscript

ROYAL SOCIETY OF CHEMISTRY

www.rsc.org/pccp

ARTICLE TYPE www. rsc.org/xxxxxx | XXXXXXXX

Monte-Carlo Simulations of Spin-Crossover Phenomena Based on a Vibronic Ising-like Model with Realistic Parameters†

Hong-Zhou Ye,‡ Chong Sun,‡ and Hong Jiang*

Received Xth XXXXXXXXXX 20XX, Accepted Xth XXXXXXXXX 20XX
First published on the web Xth XXXXXXXXXX 200X
DOI: 10.1039/b000000x

Materials with spin-crossover (SCO) properties hold great potentials in information storage and therefore have received a lot of concerns in the recent decades. The hysteresis phenomena accompanying SCO is attributed to the intermolecular cooperativity whose underlying mechanism may have a vibronic origin. In this work, a new vibronic Ising-like model in which the elastic coupling between SCO centers is included by considering harmonic stretching and bending (SAB) interactions is proposed and solved by Monte Carlo (MC) simulations. The key parameters in the new model, k_1 and k_2, corresponding to the elastic constant of the stretching and bending mode, respectively, can be directly related to the macroscopic bulk and shear modulus of the material in study, which can be readily estimated either based on experimental measurements or first-principles calculations. Using realistic parameters estimated based on density-functional theory calculations of a specific polymeric coordination SCO compound, $[Fe(pz)Pt(CN)_4] \cdot 2\,H_2O$ (pz=pyrazine), temperature-induced hysteresis and pressure effects on SCO phenomena are simulated successfully. Our MC simulations shed light on the role of the vibronic couplings in the thermal hysteresis of SCO systems, and also point out the limitations of highly simplified Ising-like models for quantitative description of real SCO systems, which will be of great value for the development of more realistic SCO models.

1 Introduction

Many transition metal complexes with d^4 to d^7 electronic configurations in octahedral coordination environments are able to undergo transition between low-spin (LS) and high-spin (HS) states, often termed as spin-crossover (SCO), under perturbations such as variation of temperature or pressure, light irradiation, applied electric or magnetic field.[1–4] It is "one of the most spectacular examples of molecular bistability", as O. Kahn remarked, and may function as "active elements in memory devices".[2] Because of their promising applications in information storage as well as their intertest in fundamental study of phase transitions, SCO systems have attracted tremendous intertest both experimentally and theoretically in past decades.[1–3,5–9] The molecular origin of SCO phenomena can be qualitatively understood based on ligand field theory,[1,2] and modern electronic structure theory have made great progress on quantitative prediction of SCO properties, including, in particular, the energy splitting between LS and HS states Δ_{HL}.[9]

One of the most spectacular features of SCO systems is the cooperativity in the SCO processes. A significant volume change usually accompanies the LS-HS transition, in which one or two electrons transfer from the non-bonding t_{2g} orbitals to the antibonding e_g orbitals. Wide hysteresis loops may be obtained as a result of strong coupling between intramolecular SCO and intermolecular interactions.[2,10,11] In this aspect, the polymeric coordination SCO materials,[2,4,12] which have stronger intermolecular interactions than supramolocular SCO compounds,[1,7] are especially promising to give wider hysteresis loops. In particular, many 2D and 3D Fe(II)-centered Hofmann-like frames have been synthesized and characterized,[13–16] some of which have shown a relatively wide hysteresis loop around room temperature.

Simulations of SCO systems based on Monte-Carlo methods have received widespread concerns, and several theoretical models have been proposed (See, e.g. Refs. 4,8 for a comprehensive review). Ising-like models, e.g., the Wajnflasz-Pick (WP) model with a site-independent and somewhat phenomenological interaction parameter J^{WP}, have been developed prosperously and explained various aspects of SCO behaviours.[17–20] More sophisticated mechanoelastic models (or atom-phonon model,[21,22] vibronic Ising-like model) such as "ball and spring" model,[23,24] attribute the phenomenological intersite interaction J in the WP model to the elastic interaction arising from molecular volume change during SCO, and therefore provides a highly simplified way to consider the couplings between spin transistion and inter-molecular vibration.[23,24] Many of these models have been generalized to

† Electronic Supplementary Information (ESI) available: [details of any supplementary information available should be included here]. See DOI: 10.1039/b000000x/

Beijing National Laboratory for Molecular Sciences, College of Chemistry and Molecular Engineering, Peking University, 100871 Beijing, China.

‡ These authors contributed equally to this work.

study spin transition in nanosized SCO compounds[4,25] by adjusting the boundary conditions used in simulations.[25,26]

In this work, we propose a new vibronic Ising-like model whose parameters can be readily estimated from first-principles calculations, and we perform Monte Carlo simulations using realistic parameters to evaluate the validity of the model for the description of thermal hysteresis behaviours in real SCO systems. The paper is organized as follows. In the next Section, we briefly review existing theoretical models and then propose the "stretching and bending" (SAB) model whose interaction parameters can be determined either experimentally or *ab initio*. Both the elastic (up to the three-body level) and the vibronic interactions are shown to be covered in this model. In Section 3, details regarding simulation strategies and parameter values used in this paper are stated. Convergence properties of the SAB model are also explored in this part. In Section 4, we first discuss the estimation of key parameters k_1 and k_2 from density functional theory (DFT) calculations of a specific ferrous Hoffman-like compound, $[Fe(pz)Pt(CN)_4]\cdot 2\,H_2O$ (pz=pyrazine) (abbreviated as Fe-pz henceforth).[27] We then demonstrate that the SAB model is able to simulate both temperature-induced hysteresis and the pressure effects on SCO phenomena. A comparison between the SAB model and the previous BAS model is also included. The final Section summarizes main findings of the work and closes the paper with some general remarks.

2 Models

2.1 Ising-like models

Consider a crystal material constituted of SCO molecules, each of which has two spin states: HS and LS, labelled with the fictitious spin variable $s=\pm 1$, respectively. The Ising-like Hamiltonian can be generally written as

$$\mathscr{H}(\{s_i\},T)=\frac{1}{2}h(T)\sum_i s_i-\frac{1}{2}\sum_{i\neq j}J(s_i,s_j)s_is_j. \qquad (1)$$

The first term in eqn (1) is given by

$$h(T)=\Delta(T)-k_{\mathrm{B}}T\ln g(T), \qquad (2)$$

$\Delta(T)$ is the intramolecular energy difference accounting for both the electronic HS-LS splitting Δ_{HL} and the temperature-dependent vibrational energy difference $\Delta E_{\mathrm{vib}}(T)$ between HS and LS states, and $g(T)$ is the ratio between the effective degeneracy in the LS and HS state, $g(T)=g_{\mathrm{HS}}(T)/g_{\mathrm{LS}}(T)$.[28] The second term in eqn (1) describes the interactions between SCO centers, and in most cases only the nearest neighbouring interaction is considered. By comparing eqn (1) to the phenomenological equation by Slichter and Drickamer,[29] one can obtain[8] the relation

$$\Delta H(T)=N_{\mathrm{A}}\Delta(T),\quad \Delta S(T)=R\ln g(T). \qquad (3)$$

In principle, eqn (3) enables us to determine the values of $\Delta(T)$ and $g(T)$ from either experimental data or *ab initio* calculations. However, only $\Delta H(T_{1/2})$ and $\Delta S(T_{1/2})$ evaluated at the transition temperature $T_{1/2}$ can be measured experimentally. On the other hand, it is also not trivial to determine temperature-dependent enthalpy and entropy from theoretical calculations, which requires the electronic energy difference at zero temperature (ΔE_{HL}) and the full vibrational (phonon) spectrum.

2.2 The WP Model

The WP model[17] is an approximation of the general Ising-like model (1), in which experimentally determinable $\Delta(T_{1/2})$, $g(T_{1/2})$ and a site-independent interaction parameter J^{WP} are used:

$$\mathscr{H}^{\mathrm{WP}}(\{s_i\},T)=\frac{1}{2}h^{\mathrm{WP}}(T)\sum_i s_i-\frac{J^{\mathrm{WP}}}{2}\sum_{\langle i,j\rangle}s_is_j, \qquad (4)$$

where $h^{\mathrm{WP}}=\Delta(T_{1/2})-k_{\mathrm{B}}T\ln g(T_{1/2})$. In this model the summation of interaction terms is restricted to nearest pairs $\langle i,j\rangle$. This approximation makes a mean-field analysis (MFA) possible, which gives a non-trivial criterion for phase transition accompanied with hysteresis[19,30,31]

$$J^{\mathrm{WP}}\geq J_{\mathrm{thresh}}=2\Delta/(z\ln g), \qquad (5)$$

where z is the coordination number.

2.3 The "Ball and Spring" Model

If lattice vibrations are added to the Ising-like model through harmonic oscillators between molecules, we have the vibronic Ising-like model. One example is the "ball and spring" (BAS) model proposed by Y. Konishi et al.[23] In this model, SCO molecules, with positions $\{\boldsymbol{r}_i\}$ as additional degrees of freedom, are described as the balls with spin-dependent radius (R_{LS} and R_{HS} for LS and HS, respectively), which are connected by elastic springs. Considering the interactions between the nearest ($\langle i,j\rangle$) and the second-nearest pairs ($\langle\langle i,j\rangle\rangle$), the Hamiltonian in the BAS model reads

$$\begin{aligned}\mathscr{H}^{\mathrm{BAS}}(\{x_i\},T)&=\frac{1}{2}h^{\mathrm{WP}}\sum_i s_i-\mathscr{H}_1^{\mathrm{BAS}}-\mathscr{H}_2^{\mathrm{BAS}},\\ \mathscr{H}_1^{\mathrm{BAS}}(\{x_i\})&=\frac{1}{2}\sum_{\langle i,j\rangle}\frac{k_1}{2}\left[r_{ij}-(R_i+R_j)\right]^2,\\ \mathscr{H}_2^{\mathrm{BAS}}(\{x_i\})&=\frac{1}{2}\sum_{\langle\langle i,j\rangle\rangle}\frac{k_2}{2}\left[r_{ij}-\sqrt{2}(R_i+R_j)\right]^2.\end{aligned} \qquad (6)$$

where $x=(\boldsymbol{r},s)$ is the four-component dynamic variable, $R_i=[(1+s_i)R_{\mathrm{HS}}+(1-s_i)R_{\mathrm{LS}}]/2$ is the radius of molecule at site i

with spin state s_i, and $r_{ij} = |\boldsymbol{r}_i - \boldsymbol{r}_j|$ is the distance between site i and j. By expanding $\mathscr{H}_1$ and $\mathscr{H}_2$ one can show that they account for the contributions from (1) spin-spin, (2) vibrational and (3) spin-vibration (vibronic) interactions. We take $\mathscr{H}_1^{\mathrm{BAS}}$ as an example:

$$\begin{aligned}\frac{k_1}{2}[r_{ij}-(R_i+R_j)]^2 = \frac{k_1}{4}(R_{\mathrm{HS}}-R_{\mathrm{LS}})^2 s_i s_j + \\ \frac{k_1}{2}(R_{\mathrm{HS}}+R_{\mathrm{LS}}-r_{ij})(R_{\mathrm{HS}}-R_{\mathrm{LS}})(s_i+s_j) + \\ \frac{k_1}{2}(R_{\mathrm{HS}}+R_{\mathrm{LS}}-r_{ij})^2 + \frac{k_1}{4}(R_{\mathrm{HS}}-R_{\mathrm{LS}})^2.\end{aligned} \tag{7}$$

The first and third term in eqn (7) depend merely on $\{s_i\}$ or $\{\boldsymbol{r}_i\}$ and characterize interactions araising from either spins or lattice distortions respectively, while the second one containing crossing term $r_{ij}s_i$ describes the spin-vibration coupling. Compared with the WP model (4), one could relate the first term in eqn (7) to J^{WP} as

$$J^{\mathrm{WP}} \sim \frac{k_1}{4}(R_{\mathrm{HS}}-R_{\mathrm{LS}})^2. \tag{8}$$

Relation (8) makes it possible to compare these two models directly: apart from spin-spin interactions, the BAS model includes vibrational and vibronic interactions as well.

Model (6) has been shown to successfully describe both temperature and pressure-induced hysteresis.[23] $\mathscr{H}_2$ may or may not be included, depending on the particular lattice structure. For example, when a simple cubic lattice is considered, it must be included to avoid structural deformation,[23] while it is not required for a hexagonal one.[24]

2.4 The "Stretching and Bending" Model

Motivated by the general picture of chemical bonding in molecular mechanics,[32] we propose that an alternative way to maintain the structure during the simulation is to assume a harmonic potential on the angle θ between two pairs of molecules sharing one common vertex. We name it as "stretching and bending" (SAB) model (Fig. 1) for reasons we would show below. The Hamiltonian is almost the same as model (6) except for $\mathscr{H}_2^{\mathrm{BAS}}$ being replaced with a bending oscillator:

$$\mathscr{H}_2^{\mathrm{SAB}}(\{\boldsymbol{r}_i\}) = \frac{1}{2}\sum_{\langle i;j,k\rangle}\frac{k_2}{2}(\theta_{ijk}-\theta_0)^2, \tag{9}$$

where $\langle i;j,k\rangle$ means that site j and k form a non-linear nearest set with respect to site i (Fig. 1), and θ_{ijk} is the corresponding angle. θ_0 is the equilibrium angle, whose value depends on the specific lattice (e.g. $\pi/2$ for cubic system, $\pi/6$ for hexagonal system etc.). In contrast to the BAS model, $\mathscr{H}_2^{\mathrm{SAB}}$ depends only on the spatial coordinates $\{\boldsymbol{r}_i\}$, which can be seen from

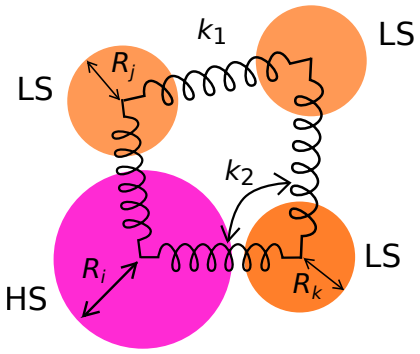

Fig. 1 A schematic illustration of the SAB model. k_1 and k_2 are Hooke's coefficients for the stretching and bending springs respectively. Two states, i.e. HS and LS, have different volumes, thus leading to a lattice distortion and then elastic interactions when SCO happens.

the explicit expression of θ_{ijk},

$$\theta_{ijk} = \arccos\left(\frac{r_{ij}^2 + r_{ik}^2 - r_{jk}^2}{2r_{ij}r_{ik}}\right). \tag{10}$$

Thus interactions arising from spins or spin-vibration coupling are absent in the bending oscillator.

A great advantage of the SAB model is that both k_1 and k_2 are of definite physical significance and can be related to the macroscopic bulk modulus K and shear modulus G, respectively

$$K = \frac{k_1}{3v_0^{1/3}}, \qquad G = \frac{4k_2}{v_0}, \tag{11}$$

where v_0 is the equilibrium volume of the unit cell (for derivations see Appendix A). Although experimental data for the moduli of SCO systems are still quite scarce, they can be readily determined from the equation of state (EOS) calculated by density functional theory (DFT). In addition, the SAB model has also the advantage that it can be straightforwardly generalized to treat lattice structures with any symmetry, not limited to the cubic one, and therefore allows for more realistic modeling of real SCO compounds, which usually have much lower symmetry than the ideal cubic one.[12]

3 Computational Details

In this section we give some details on how the MC simulations based on the SAB model are performed in practice and discuss its convergence properties.

We consider a 3D periodic simple cubic lattice with size $N = n^3$ ($n = 16$ unless stated otherwise) and length $L = 2nR$ at each side, with $R = R_{\mathrm{LS}}$ or R_{HS}, corresponding, respectively, to a pure LS or HS initial state. We perform the MC simulation in the Gibbs (N, p, T)-ensemble, and we have adopted a

simulation scheme that is very similar to that used by Konishi *et al* in Ref. 23. In particular, a complete Monte-Carlo step (MCS) is constituted of:

(i) Choose randomly a candidate site i with $x_i = (s_i, \boldsymbol{r}_i)$.

(ii) Choose a candidate spin $s_i' = +1$ or -1 for it, with the probability $g/(g+1)$ and $1/(g+1)$ respectively.

(iii) Choose a candidate position $\boldsymbol{r}_i' = \boldsymbol{r}_i + \delta\boldsymbol{\xi}$, where $\delta = 0.005L$, and ξ_α ($\alpha = x,y,z$) is randomly chosen from $[-1.0, 1.0]$.

(iv) Accept x_i' according to the Metropolis scheme

$$P(x_i \to x_i') = \min\left[1, \exp(-\Delta\mathscr{H}/k_{\mathrm{B}}T)\right], \qquad (12)$$

where $x_i' = (s_i', \boldsymbol{r}_i')$ and $\Delta\mathscr{H} = \mathscr{H}^{\mathrm{SAB}}(x_i', T) - \mathscr{H}^{\mathrm{SAB}}(x_i, T)$.

(v) Repeat (i) to (iv) N times.

(vi) Choose a candidate length $L' = L + \gamma\zeta$ with $\gamma = 0.08nR_{\mathrm{LS}}$ and ζ randomly chosen from $[-1.0, 1.0]$.

(vii) Update L according to the Metropolis scheme

$$P(L \to L') = \min\left[1, \exp(-\Delta W/k_{\mathrm{B}}T)\right], \qquad (13)$$

where

$$\Delta W = \Delta\mathscr{H} + p(V' - V) - NT\ln\left(\frac{V'}{V}\right). \qquad (14)$$

Ensemble average of the HS state fraction, x_{HS}, is obtained through averaging over the last ten MCSs.

For a given set of parameters, we run MC simulations for a series of temperatures around $T_{1/2}$. At each temperature the system is initialized by setting all sites in the LS and HS state for the heating and cooling process, respectively, and is equilibrized by a certain number of MCSs, termed as the sweeping rate (MCS/K), which, as discussed below, has significant effects on the simulated hysteresis behaviors.

Most energetic parameters in the simulations used below are expressed in terms of Kelvin. For quantities with unit of energy (i.e. Δ, J and k_2), dividing them by k_{B} completes the transform. k_1 needs some special treatment as followed:

$$\begin{aligned}\mathscr{H} &\sim k_1[r_{ij} - (R_i + R_j)]^2 \\ &= k_1 {R_{\mathrm{LS}}}^2\left[\frac{r_{ij}}{R_{\mathrm{LS}}} - \left(\frac{R_i}{R_{\mathrm{LS}}} + \frac{R_j}{R_{\mathrm{LS}}}\right)\right]^2 \\ &= k_1'[r_{ij}' - (R_i' + R_j')]^2,\end{aligned} \qquad (15)$$

where by choosing R_{LS} as the unity of length, we have $k_1' = k_1 {R_{\mathrm{LS}}}^2$ possessing the unit of energy and thus can be transformed into Kelvin. In the following, we use k_1, r and R to denote these "reduced" quantity k_1', r' and R' for simplicity. Pressure p can be treated in a very similar manner. In the following simulations, if not specified otherwise, we take typical experimentally measured $\Delta H = 15\,\mathrm{kJ\cdot mol^{-1}}$, $\Delta S = 60\,\mathrm{J\cdot mol^{-1}\cdot K^{-1}}$ (corresponding to $\Delta = 1800\,\mathrm{K}$ and $g = 1360$) and ambient pressure $p = 1\,\mathrm{atm}$ (corresponding to $p = 2.6\times10^{-4}\mathrm{K}$). We set $R_{\mathrm{LS}} = 4.0\mathring{A}$ and $R_{\mathrm{HS}}/R_{\mathrm{LS}} = 1.1$ for the effective radii of the SCO molecule in the LS and HS state, estimated in terms of the crystal structure of the Fe-pz compound.[16] We note that consistent values of those parameters should be used in order to obtain reasonable simulation results.[33]

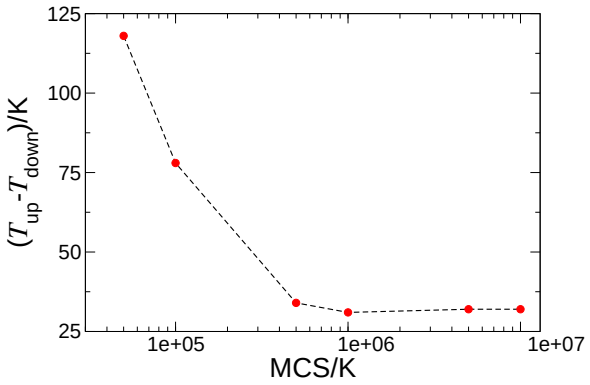

Fig. 2 Hysteresis loop widths versus sweeping rates using the SAB model. $k_1 = 7.2\times10^4\,\mathrm{K}$ and $N = 16^3$.

One more technical thing is worth discussing here. In simulating hysteresis phenomena, it is essential to require that the results be stable under an increase in the number of MCSs, or equivalently speaking, under slowing down the sweeping rate (MCS/K). This basic requisite is by no means trivial. For example, hysteresis loops obtained from simulations based on the simple WP model will often shrink if one slows the sweeping rate (See ESI† for details), thus being unable to generate a stable simulation result. However, we show here that the SAB model is, if not free of, able to partially fix this convergence problem. To demonstrate it, we compare the widths of hysteresis loop versus the sweeping rate using this model. The results are illustrated in Fig. 2. One can clearly see that the SAB model can lead to a stable hysteresis loop as long as a large enough but still computationally bearable number of MCS/K is used (e.g. 10^6).

4 Results and Discussions

4.1 *Ab Initio* Estimation of k_1 and k_2

We first discuss how the realistic values of k_1 and k_2 can be estimated based on DFT calculations. For 3D simple cubic systems, k_1 and k_2 are related to the following two equations of states

$$E_{\mathrm{el}}(x) = \frac{3}{2}k_1 v_0^{2/3}(x-1)^2, \quad E_{\mathrm{el}}(\gamma) = 2k_2(\gamma - \pi/2)^2, \quad (16)$$

where E_{el} and v_0 are the total electronic energy and equilibrium volume of a unit cell respectively, $x = (v/v_0)^{1/3}$, and γ

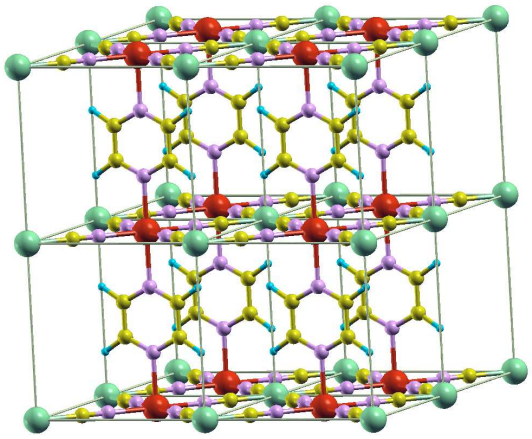

Fig. 3 Schematic illustration of the crystal structure of $[Fe(pz)Pt(CN)_4]\cdot 2H_2O$ (pz=pyrazine). Fe (red), Pt (green), C (yellow), N (purple), H (blue). Water molecules are removed for the sake of conciseness.

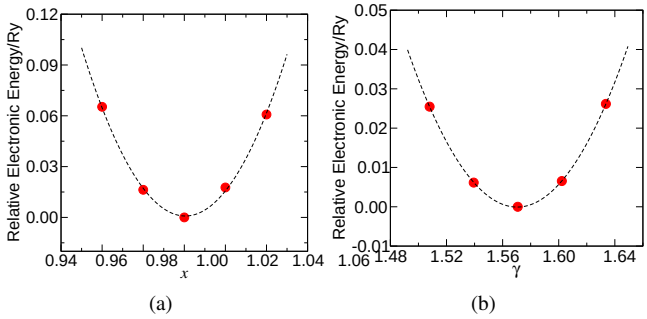

Fig. 4 DFT calculation results of the total electronic energy versus (a) lattice volume and (b) angle γ using PBEsol for $[Fe(pz)Pt(CN)_4]\cdot 2H_2O$ in LS state. Dashed lines are fitting curves according to eqn (16).

is one of the lattice angles (for derivations see Appendix A). Using eqn (16), we can now estimate the approximate values of k's for the Fe-pz compound (see Fig. 3 for the structure). We conducted DFT calculations for $E_{\rm el}(x)$ and $E_{\rm el}(\gamma)$ using the PBEsol functional,[34] as implemented in the Quantum ESPRESSO package,[35] and the results are shown in Fig. 4. Quadratic fittings according to eqn (16) of calculated values result in good consistency and give estimated values for k's in our model $k_1 \approx 1.2\times 10^6\,$K and $k_2 \approx 5.5\times 10^5\,$K. Thus a ratio

$$k_1/k_2 \approx 2 \qquad (17)$$

holds. We will use this ratio in all of the following simulations throughout this paper.

4.2 Temperature-Induced SCO Hysteresis

Based on the estimation of k_1 and k_2 in the SAB model, we can now exploit its ability to simulate hysteresis phenomena. First we tackle the temperature-induced SCO under ambient pressure. In order to estimate the appropriate sweeping rates, we depict HS fraction $x_{\rm HS}$ versus MCS for various values of k_1 at several representative temperatures (Fig. 5). When k_1 is small, e.g. (a) and (b), a gradual increase of stable $x_{\rm HS}$ is observed as temperature goes up, which indicates a gradual phase transition curve $x_{\rm HS}(T)$. On the other hand, when k_1 is large, e.g. (c) and (d), no intermediate values between 0 and 1 of stable $x_{\rm HS}$ are observed and abrupt phase transitions with hysteresis are expected.

After preparing all of these, we study the shapes of $x_{\rm HS}(T)$ curves with respect to different interaction strength k's, and the results are depicted in Fig. 6. As we have expected, $k_1 = 1.8\times 10^4\,$K and $3.6\times 10^4\,$K result in gradual changes, while $k_1 \geq 7.2\times 10^4\,$K give abrupt phase transitions with hysteresis. The case of $k_1 = 5.4\times 10^4\,$K seems to be somewhat critical, also abrupt but without loop. $k_1 = 1.3\times 10^5$ is also special since the HS state continues to dominate at very low temperature, indicating a metastable HS state and incomplete SCO. The change of $x_{\rm HS}(T)$ curves from being gradual to abrupt with increasing interactions follows the concept of "generic sequence" suggested by Y. Konishi.[23]

It is worth pointing out that, in the simulations above we

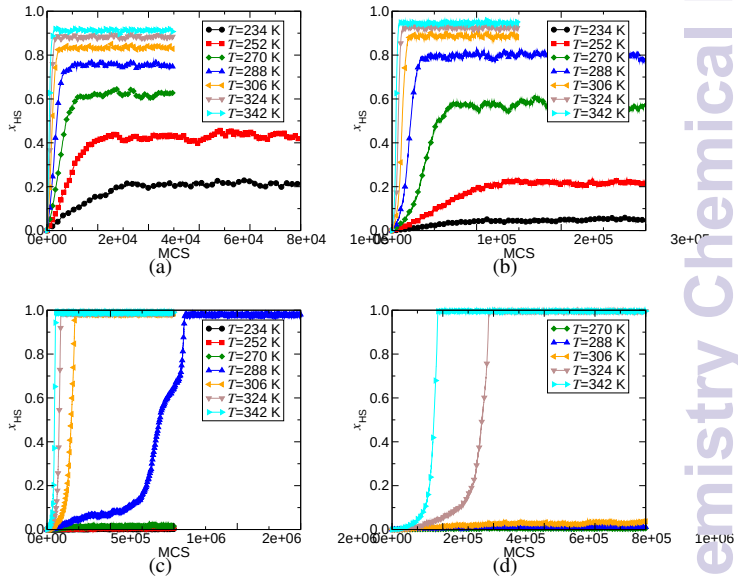

Fig. 5 Convergence tests of (a) $k_1 = 1.8\times 10^4\,$K, (b) $3.6\times 10^4\,$K, (c) $7.2\times 10^4\,$K and (d) $9.0\times 10^4\,$K. It is easy to see that more MCSs are required when (i) k_1 is larger, and (ii) temperatures are close to phase transition.

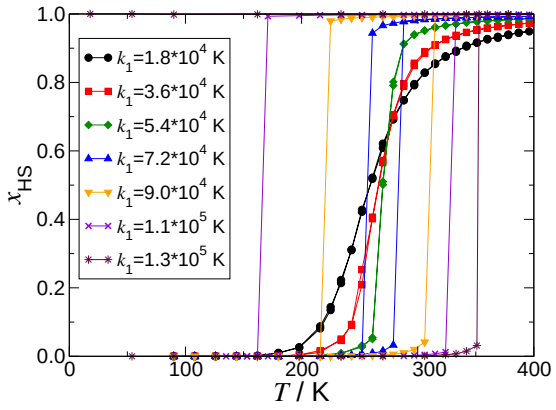

Fig. 6 Phase transition curves $x_{\mathrm{HS}}(T)$ with $k_1 = 1.8 \times 10^4$ K (black circle), 3.6×10^4 K (red square), 5.4×10^4 K (green diamond), 7.2×10^4 K (blue triangle-up), 9.0×10^4 K (orange triangle-down), 1.1×10^5 K (purple cross) and 1.3×10^5 K (brown star).

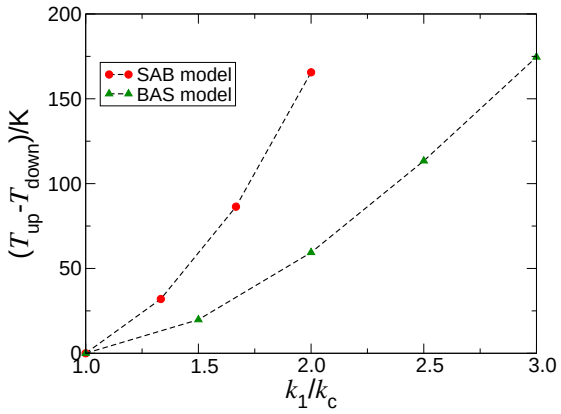

Fig. 7 Variation of hysteresis loop widths with respect to various k_1 for the SAB (red circle) and the BAS (green triangle) model. All parameter values follow the discussion in simulation details except $k_1 = 10k_2$ are employed for the BAS model.[23]

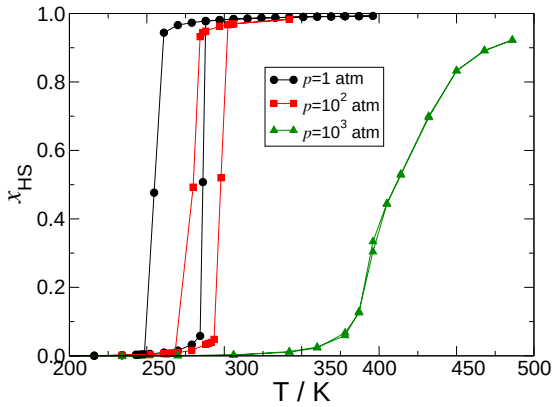

Fig. 8 Simulating pressure effects on hysteresis loop with the SAB model for the case $k_1 = 7.2 \times 10^4$ K.

only use the ratio (17) for k_1 and k_2 obtained from DFT calculations, and the absolute values of k_1 and k_2 at which significant hysteresis loops emerge are almost 20 times smaller than those estimated based on DFT calculations. If the latter are used, i.e. $k_1 = 1.2 \times 10^6$ K and $k_2 = 5.5 \times 10^5$ K, a much wider loop is expected accompanied with a HS metastable state in the low temperature regime. Experimentally the Fe-pz compound we consider exhibits a hysteresis loop of about 20 K,[36] which corresponds to $k_1 \sim 7 \times 10^4$ K in our simulation. The discrepancy between simulation and experiment is probably due to the fact that the SAB model considers vibronic intermolecular couplings in a highly simplified way. One of the features missing in our SAB model is the anisotropy (i.e. tetragonal rather than cubic symmetry) of the Fe-pz compound, which, by considering different elastic constants k_1 along different directions, can be incorporated in a straightforward way.

For comparison, we also conduct MC simulations based on the BAS model of Ref. 23. Using the same values for all the parameters[33] except for k_2, which in the BAS model uses $k_2 = k_1/10$ as in Ref. 23, we obtain transition curves qualitatively similar to Fig. 6 (See ESI† for details). Quantitatively speaking, however, the results from the two models are significantly different. From Fig. 6 and ESI†, we can see that the critical value of k_1 at which the spin transition is abrupt but without hysteresis, denoted as k_c, is almost three times different in the two models, with $k_c^{\mathrm{SAB}} \approx 5.4 \times 10^4$ K and $k_c^{\mathrm{BAS}} \approx 1.8 \times 10^4$ K respectively. In addition, Fig. 7 shows the width of the hysteresis loop, $T_{\mathrm{up}} - T_{\mathrm{down}}$, as a function of k_1/k_c obtained in the two models, which shows that the hysteresis width increases more rapidly as a function of k_1 in the SAB model than that in the BAS model. From these comparisons we can see that the third term in eqn. 6, which is the only difference between the BAS and SAB model, is physically very important, in contrast to the original intention of introducing the term as a technical trick to maintain the cubic symmetry of the simulation lattice.[23] Such insights to the models can be obtained only if one insists on using realistic parameters as much as possible.

4.3 Pressure Effects on SCO Hysteresis

Pressure is often used experimentally to probe the spin transition mechanism in SCO compounds.[12] Since the pressure is an adjustable parameter in the SAB model, we can investigate the pressure effects on hysteresis loops. We choose the case $k_1 = 7.2 \times 10^4$ K in the above simulations and consider its behaviours when increasing p from 1 atm to 10^3 atm. As shown in Fig. 8, the transition temperature $T_{1/2}$ shifts towards high temperature as the pressure increases; in the meantime

the width of the hysteresis loop is reduced at high pressure and finally vanishes, similar to the previously reported results in the BAS model.[23] The effect of pressure on $T_{1/2}$, which is consistent with experimental observations,[12] can be easily rationalized since the LS-HS transition is accompanied by an increase of the volume and therefore increasing pressure suppresses the transition. The cause for the diminishment of the hysteresis loop at high pressure is less straightforward, and is actually in disagreement with experiment.[12] Experimental findings about the effects of pressure on hysteresis are highly system-dependent, but in most cases the hysteresis loop is well maintained under high pressure.[12] The discrepancy between theory and experiment again indicates the limitation of the highly simplified vibronic Ising-like models like BAS and SAB.

5 Concluding remarks

In summary, we propose a new vibronic Ising-like model that accounts for spin-vibration couplings by considering the harmonic stretching and bending interactions based on the previously reported ball-and-spring model.[23] Within an acceptable amount of simulation time, MC simulations based on the SAB model are able to produce stable and reproducible hysteresis loops. Key parameters, i.e. the elastic constants k_1 and k_2, can be directly related to the macroscopic bulk and shear modulus of the material in study, and hence can be estimated from either experimental values or *ab initio* calculations. DFT calculations on a specific polymeric coordination SCO compound, $[Fe(pz)Pt(CN)_4]\cdot 2\,H_2O$, is performed and give an estimation of the ratio k_1/k_2, with which we successfully simulate the temperature-induced hysteresis and pressure effects on SCO phenomena. A comparison between the SAB and the BAS model indicates that the two models, although formally similar and leading to qualitatively same hysteresis behaviors, are quantitatively very different.

Regarding the validity of such vibronic Ising-like models to describe real systems, we note that only a qualitative consistency with experiment is achieved when using the values of k_1 and k_2 estimated based on DFT calculations. Apart from the structural anisotropy that is neglected in our simulation, the SAB model itself may well be intrinsically over-simplified. The limitations of such models become transparent only we use realistic parameters estimated based on first-principles calculations.

Acknowledgement

We would like to thank Mr. Zehua Chen for many useful suggestions on our codes. This project was supported by the Hui-Chun Chin and Tsung-Dao Lee Chinese Undergraduate Research Endowement (CURE), National Natural Science Foundation of China (Projects No. 20973009, 21373017), National Basic Research Program of China (2013CB933400) and Ministry of Education of China (20120001110063).

A Derivation of Eq. (11) and (16)

Here we show the derivation details for Eqs. (11) and (16). For the bulk modulus K, consider a homogeneous expansion of a simple cubic lattice which has volume V_0 at equilibrium and now V. The total electronic energy corresponding to this volume change is:

$$\begin{aligned} E_{\mathrm{el}}(V) &= 3N\times\frac{k_1}{2}\left[\left(\frac{V}{N}\right)^{1/3}-\left(\frac{V_0}{N}\right)^{1/3}\right]^2 \\ &= \frac{3}{2}Nk_1\left(\frac{V_0}{N}\right)^{1/3}\left[\left(\frac{V}{V_0}\right)^{1/3}-1\right]^2 \\ &= \frac{3}{2}Nk_1v_0^{2/3}(x-1)^2 \end{aligned} \tag{18}$$

where $v_0 = V_0/N$ is the unit cell volume and $x = (V/V_0)^{1/3}$ is the stretching ratio in length. This is actually the EOS of volume change appeared in (16). Substitute (18) into the definition of bulk modulus $K = V\mathrm{d}^2E/\mathrm{d}V^2$, we have

$$K = \frac{1}{3}\left(\frac{N}{V}\right)^{1/3}\left[2\left(\frac{V_0}{V}\right)^{1/3}-1\right]k_1. \tag{19}$$

At equilibrium, $V = V_0$ and hence $K = k_1/(3v_0^{1/3})$ holds.

For the shear modulus G, consider a small displacement of γ from equilibrium position $\gamma_0 = \pi/2$. The total electronic energy is

$$E_{\mathrm{el}}(\gamma) = 4N\times\frac{k_2}{2}(\gamma-\gamma_0)^2, \tag{20}$$

which is the EOS of γ in (16). According to the definition of shear modulus, we have

$$G = \frac{1}{\gamma-\gamma_0}\frac{\mathrm{d}E}{\mathrm{d}\gamma} = 4Nk_2, \tag{21}$$

which completes the derivations for (11).

References

1 *Spin crossover in transition metal compouns, vol 1-3*, ed. H. A. Gütlich and H. A. Goodwin, Springer, Berlin, 2004.
2 O. Kahn and C. J. Martinez, *Science*, 1998, **279**, 44.
3 R. Boča and W. Linert, *Monatsh. für Chem.*, 2003, **134**, 199.
4 A. Bousseksou, G. Molnar, L. Salmon and W. Nicolazzi, *Chem. Soc. Rev.*, 2011, **40**, 3313 – 3335.
5 P. Gütlich, A. Hauser and H. Spiering, *Angew. Chem. Int. Ed.*, 1994, **33**, 2024 – 2054.
6 M. A. Halcrow, *Chem. Soc. Rev.*, 2011, **40**, 4119 – 4142.

7 J. Tao, R.-J. Wei, R.-B. Huang and L.-S. Zheng, *Chem. Soc. Rev.*, 2012, **41**, 703 –737.

8 J. Pavlik and R. Boča, *Eur. J. Inorg. Chem.*, 2013, **31**, 697 – 709.

9 H. Paulsen, V. Schünemann and J. A. Wolny, *Eur. J. Inorg. Chem.*, 2013, 628 – 641.

10 J. A. Real and M. C. GaMuñoz, M. C.ñoz, *Coord. Chem. Rev.*, 2003, **236**, 121 – 141.

11 W. Vreugdenhill, J. H. V. Diemen, R. A. G. D. Graaff, J. G.Haasnoot, J. Reedijk, A. M. V. der Kraan, O. Kahn and J. Zarmbowitch, *Polyhedron*, 1990, **9**, 2971.

12 M. C. Muñoz and J. A. Real, *Coord. Chem. Rev.*, 2011, **255**, 2068.

13 T. Kitazawa, Y. Gomi, M. Takahashi, M. Takeda, M. Enomoto, A. Miyazaki and T. Enoki, *J. Mater. Chem.*, 1996, **6**, 119.

14 G. Molnar, T. Kitazawa, L. Dubrovinsky, J. J. McGarvery and A. Bousseksou, *J. Phys.: Condens. Matt.*, 2004, **16**, 1129.

15 K. Hosoya, T. Kitazawa, M. Takahashi, M. Takeda, J. F. Meunier, G. Molnár and A. Bousseksou, *J. Phys. Chem. Chem. Phys.*, 2003, **5**, 1682.

16 V. Niel, M. C. M. J. M. Martinez-Agudo, A. B. Gaspar and J. A. Real, *Inorg. Chem.*, 2001, **40**, 3838.

17 J. Wajnflasz and R. Pick, *J. Phys. Colloque*, 1971, **32**, C1.

18 H. Bolvin and O. Kahn, *Chem. Phys*, 1995, **192**, 295.

19 M. Nishino, K. Boukheddaden, S. Miyashita and F. Varret, *Phys. Rev. B*, 2003, **68**, 224402.

20 A. Bousseksou, J. Nasser, J. Linares, K. Boukheddaden and F. Varret, *J. Phys. I France*, 1992, **2**, 1381.

21 J. A. Nasser, *Eur. Phys. J. B*, 2001, **21**, 3.

22 K. Boukheddaden, S. Miyashita and M. Nishino, *Phys. Rev. B*, 2007, **75**, 094112.

23 Y. Konishi, H. Tokoro, M. Nishino and S. Miyashita, *Phys. Rev. Lett.*, 2008, **100**, 067206.

24 L. Stoleriu, P. Chakraborty, A. Hauser, A. Stancu and C. Enachescu, *Phys. Rev. B*, 2011, **84**, 134102.

25 M. Mikolasek, G. Félix, W. Nicolazzi, G. Molnár, L. Salmon and A. Bousseksou, *New J. Chem.*, 2014, **38**, 1834.

26 I. Gudyma, A. Maksymov and C. Enachescu, *Phys. Rev. B*, 2014, **89**, 224412.

27 V. Niel, J. M. Martinez-Agudo, M. C. Muñoz, A. B. Gaspar and J. A. Real, *Inorg. Chem.*, 2001, **40**, 3838 – 3839.

28 S. Miyashita, Y. Konishi, H. Tokoro, M. Nishino, K. Boukheddaden and F. Varret, *Prog. Theo. Phys.*, 2005, **114**, 719.

29 C. P. Slichter and H. G. Drickamer, *J. Chem. Phys.*, 1972, **56**, 2142.

30 K. Boukheddaden, I. Shteto, B. Hôo and F. Varret, *Phys. Rev. B*, 2000, **62**, 14796.

31 F. Varret, S. A. Salunke, K. Boukheddaden, A. Bousseksou, E. Codjovi, C. Enachescu and J. Linares, *C. R. Chimie*, 2003, **6**, 385.

32 A. R. Leach, *Molecular Modeling: Principles and Applications*, Prentice Hall, 2001.

33 According to eqn (3), a typical entropy leads to $g \approx 1000$. In Ref. 23 however, the author assumes $g = 20$, i.e. only electronic contribution to degeneracy is considered. As a result, a very large pressure $p = 0.01$ (corresponding to $p \approx 40$ atm) must be used, while in our simulation both g and p are related to realistic parameters directly.

34 J. P. Perdew, A. Ruzsinszky, G. I. Csonka, O. A. Vydrov, G. E. Scuseria, L. A. Constantin, X. Zhou and K. Burke, *Phys. Rev. Lett.*, 2008, **100**, 136406.

35 P. Giannozzi *et al.*, *J.Phys.:Condens.Matter*, 2009, **21**, 395502.

36 S. Bonhommeau, G. Molnar, A. Galet, A. Zwick, J. A. Real, J. J. McGarvMcGarvery and A. Bousseksou, *Angew. Chem. Int. Ed.*, 2005, **44**, 4069 – 4073.

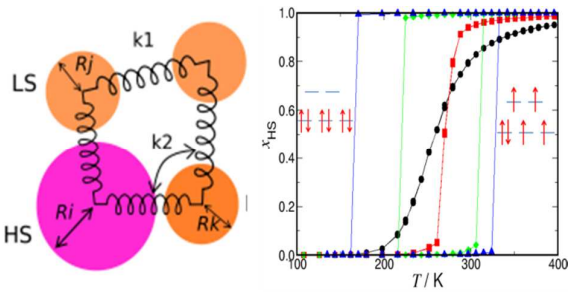

A new vibronic Ising-like model considering harmonic stretching-and-bending intermolecular interactions with realistic parameters describes thermal hysteresis in spin-crossover phenomena well.